

Sticking Transition in a Minimal Model for the Collisions of Active Particles in Quantum Fluids

Vishwanath Shukla,^{1,2,*} Marc Brachet,^{3,†} and Rahul Pandit^{2,‡}

¹*Laboratoire de Physique Statistique de l'École Normale Supérieure, 24 Rue Lhomond, 75231 Paris, France*

²*Centre for Condensed Matter Theory, Department of Physics,
Indian Institute of Science, Bangalore 560012, India.*

³*Laboratoire de Physique Statistique de l'École Normale Supérieure,
associé au CNRS et aux Universités Paris VI et VII, 24 Rue Lhomond, 75231 Paris, France*

(Dated: June 1, 2021)

Particles of low velocity, travelling without dissipation in a superfluid, can interact and emit sound when they collide. We propose a minimal model in which the equations of motion of the particles, including a short-range repulsive force, are self-consistently coupled with the Gross-Pitaevskii equation. We use this model to demonstrate the existence of an effective superfluid-mediated attractive interaction between the particles; and we study numerically the collisional dynamics of particles as a function of their incident kinetic energy and the length-scale of the repulsive force. We find a transition from almost elastic to completely inelastic (sticking) collisions as the parameters are tuned. We find that aggregation and clustering result from this sticking transition in multi-particle systems.

PACS numbers: 47.55.Kf, 47.37.+q, 67.25.dg

Keywords: Active particles; Superfluidity; Quantum fluids

Studies of an assembly of particles in a superfluid have a rich history [1]. This challenging problem is of relevance to recent experiments on particles in superfluid helium [2–6] and impurities in cold-atom Bose-Einstein condensates (BECs) [7]. Its understanding requires models and techniques from the physics of quantum fluids with state-of-the-art methods from theoretical and numerical studies of turbulence. In contrast to particles moving through a viscous fluid, particles move through a zero-temperature superfluid without dissipation, so long as they travel at speeds lower than the critical speed above which the particles shed quantum vortices [8–10]. The motion of a single particle, which is affected by the superflow and acts on it too, has been studied in Ref. [11] in a Gross-Pitaevskii (GP) superfluid. We refer to this as an *active particle*.

We go well beyond earlier studies [11–13] of this problem by developing a minimal model. We introduce *active and interacting* particles in the Gross-Pitaevskii Lagrangian that describes a weakly interacting superfluid at zero temperature. By using this model we show that, even if particles move through the superfluid at subcritical speeds, they can dissipate energy when they collide, because a two-particle collision excites sound waves; clearly the coefficient of restitution $e < 1$, for such a collision. Furthermore, we demonstrate that there is a superfluid-mediated attraction between the particles. We calculate this attraction both approximately, via a Thomas-Fermi approximation, and numerically, from a direct numerical simulation (DNS) of the Gross-Pitaevskii Equation (GPE). We show that the interplay between the short-range (SR) particle repulsion, which we have included in our Lagrangian, and the superfluid-mediated (SM) attraction leads to a *sticking* transition

at which the coefficient of restitution e for two-particle collisions vanishes. We develop a simple, mean-field theory for this transition and we compare it with our DNS results. Furthermore, we elucidate the rich dynamical behaviors of (a) two-particle collisions in the superfluid, when the impact parameter b is nonzero, and (b) assemblies of particles, which aggregate because of the SM attraction.

To study the dynamics of particles in a Bose superfluid, we propose the Lagrangian

$$\begin{aligned} \mathcal{L} = & \int_{\mathcal{A}} \left[\frac{i\hbar}{2} \left(\psi^* \frac{\partial \psi}{\partial t} - \psi \frac{\partial \psi^*}{\partial t} \right) - \frac{\hbar^2}{2m} \nabla \psi \cdot \nabla \psi^* + \mu |\psi|^2 \right. \\ & \left. - \frac{g}{2} |\psi|^4 - \sum_{i=1}^{\mathcal{N}_0} V_{\mathcal{P}}(\mathbf{r} - \mathbf{q}_i) |\psi|^2 \right] d\mathbf{r} + \frac{m_o}{2} \sum_{i=1}^{\mathcal{N}_0} \dot{q}_i^2 \\ & - \sum_{i,j,i \neq j}^{\mathcal{N}_0, \mathcal{N}_0} \frac{\Delta_E r_{SR}^{12}}{|\mathbf{q}_i - \mathbf{q}_j|^{12}}, \end{aligned} \quad (1)$$

where ψ is the complex, condensate wave function, ψ^* its complex conjugate, \mathcal{A} the simulation domain, g the effective interaction strength, m the mass of the bosons, μ the chemical potential, $V_{\mathcal{P}}$ the potential that we use to represent the particles, and \mathcal{N}_0 the total number of particles with mass m_o . The last term in Eq. (1) is the SR repulsive, two-particle potential; we treat Δ_E and r_{SR} as parameters.

The Lagrangian (1) yields the GPE

$$i\hbar \frac{\partial \psi}{\partial t} = -\frac{\hbar^2}{2m} \nabla^2 \psi - \mu \psi + g |\psi|^2 \psi + \sum_{i=1}^{\mathcal{N}_0} V_{\mathcal{P}}(\mathbf{r} - \mathbf{q}_i) \psi; \quad (2)$$

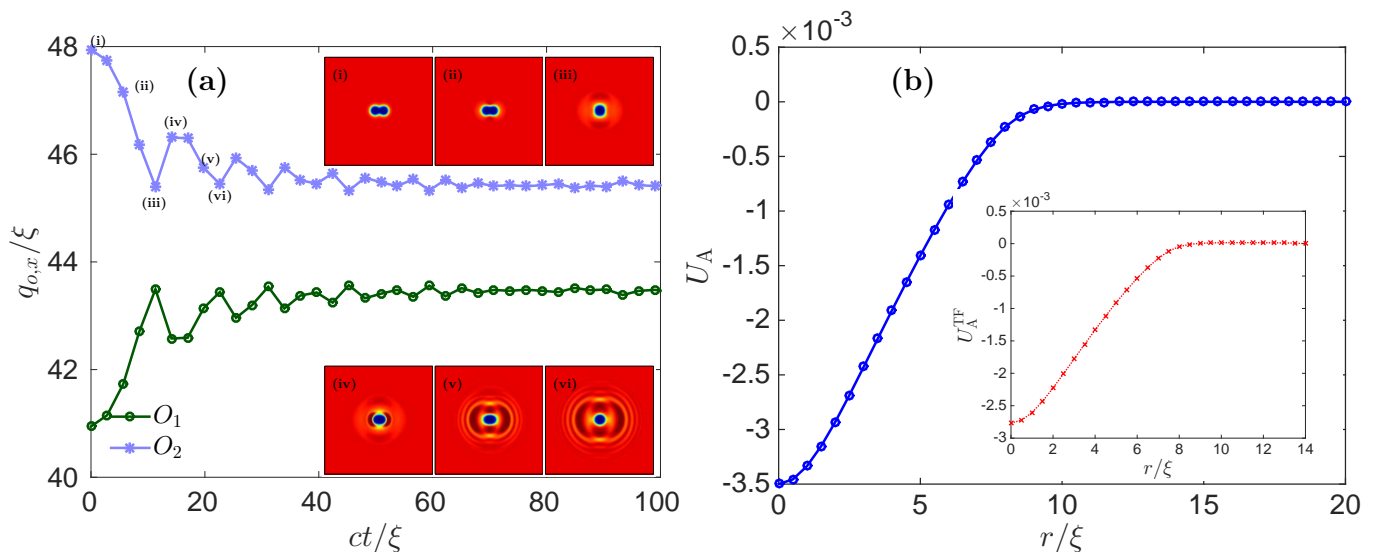


FIG. 1. (Color online) **Superfluid-mediated attractive potential:** (a) Plot of the particle ($\mathcal{M} = 1$) positions $q_{o,x}$ versus the scaled time ct/ξ . Inset: the sequence of the collision events shown via the pseudocolor plots of the density field $\rho(\mathbf{r})$ (the particles appear as blue disks in which $\rho = 0$); particles are released from rest, with an initial separation $r_0 = 7\xi$, they undergo multiple collisions with the generation of sound waves in the wake of this collision; and they form a bound state with $r \simeq r_{\text{SR}}$. (b) Plot of the superfluid-mediated attractive potential U_A versus the separation between the particles r/ξ obtained from our DNSs; the inset shows the same plot, but evaluated by using the Thomas-Fermi approximation Eq. (7).

and the equation of motion for the particle i

$$m_o \ddot{\mathbf{q}}_i = \mathbf{f}_{o,i} + \mathbf{f}_{\text{SR},i}, \quad (3)$$

where

$$\mathbf{f}_{o,i} = \int_{\mathcal{A}} |\psi|^2 \nabla V_{\mathcal{P}} d\mathbf{r}; \quad (4)$$

$\mathbf{f}_{\text{SR},i}$ arises from the SR repulsive potential (the last term in Eq. (1)). In the absence of any external force, the total energy of this system is conserved. Moreover, the dynamical evolution of the coupled set of Eqs. (2)-(3) conserves the total momentum and the number of bosons, which constitute the superfluid. We can express the GP in terms of hydrodynamical variables by using the Madelung transformation $\psi(\mathbf{r}, t) = \sqrt{\rho(\mathbf{r}, t)/m} \exp(i\phi(\mathbf{r}, t))$, where $\rho(\mathbf{r}, t)$ and $\phi(\mathbf{r}, t)$ are the density and phase fields, respectively; the superfluid velocity is $\mathbf{v}(\mathbf{r}, t) = (\hbar/m) \nabla \phi(\mathbf{r}, t)$, which shows that the motion is irrotational in the absence of any vortices. We represent a particle by the Gaussian potential $V_{\mathcal{P}} = V_o \exp(-r^2/2d_p^2)$; here V_o and d_p are the strength of the potential and its width, respectively. The particle displaces some superfluid with an area of the order of the particle area; we denote the mass of the displaced superfluid by m_f . We use the ratio $\mathcal{M} \equiv m_o/m_f$ to define three types of particles: (1) heavy ($\mathcal{M} > 1$), (2) neutral ($\mathcal{M} = 1$), and (3) light ($\mathcal{M} < 1$).

To solve Eq. (2)-(3) numerically, we use a pseudospectral method with the 2/3-dealiasing rule [14, 15], on a 2D, periodic, computational domain of side $L = 2\pi$, i.e.,

$\mathcal{A} = L^2$; we use a fourth-order, Runge-Kutta scheme for time marching. We work with the quantum of circulation $\kappa \equiv h/m \equiv 4\pi\alpha_0$, speed of sound $c = \sqrt{2\alpha_0 g \rho_0}$, and healing length $\xi = \sqrt{\alpha_0 / (g\rho_0)}$. In all our calculations, we set $\rho_0 = 1$, $c = 1$, and $\xi = 1.44 dx$, where $dx = L/N_c$, $N_c = 128$ is the number of collocation points, $\mu = g$, $V_o = 10g$, $d_p = 1.5\xi$, and $\Delta_E = 0.062$. [See the Supplemental Material [16] for details.]

We first examine a head-on, two-particle collision. We prepare an initial state with two neutral particles, at rest, separated by $r_0 = 7\xi$ in the superfluid [17]. We evolve this state by using the GPE in the presence of the SR repulsion between the particles, with $r_{\text{SR}} = 1.5\xi$, after they are released from rest at $t = 0$. In Fig. 1(a) we plot the particle positions versus the scaled time ct/ξ . In the insets of Fig. 1(a), we show pseudocolor plots of $\rho(\mathbf{r})$ at times labeled (i)-(vi); these plots show sound waves after the collision between the particles, which appear as blue disks with $\rho = 0$. We see that the particles accelerate towards each other and stop on collision, when the separation $r \simeq r_{\text{SR}}$; and then their motion is reversed, but they do not escape to infinity and undergo multiple collisions, which are accompanied by acoustic emission, until they lose their initial kinetic energy and they stick to form a bound pair; i.e., we have an inelastic collision (see the spatiotemporal evolution in Video M1, Supplemental Material [16]).

To characterize the SM attractive potential between the particles, we write the total energy contained in the

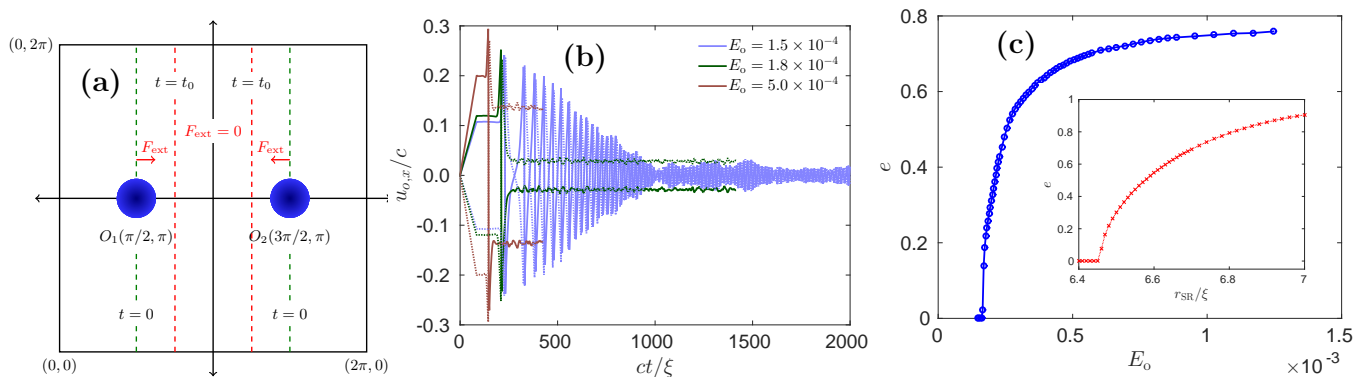


FIG. 2. (Color online) **Head-on collisions:** (a) Schematic diagram outlines the initial configuration and the procedure that we use to study the head-on collision between two particles (blue disks). (b) Plots of the particle velocity $u_{o,x}$ versus t following a head-on collisions between two heavy particles ($\mathcal{M} = 7.5$) for three different values of the incident kinetic energy E_o , at $r_{\text{SR}} = 1.5\xi$. (c) Plot of the coefficient of restitution e (Eq. (8)) versus E_o , for the head-on collision between two heavy particles ($\mathcal{M} = 7.5$). The inset shows e versus r_{SR}/ξ , but for two neutral particles ($\mathcal{M} = 1$).

superfluid field as

$$E_{\text{F}} = \frac{1}{\mathcal{A}} \int_{\mathcal{A}} \left[\frac{\hbar^2}{2m} |\nabla\psi|^2 + \frac{g}{2} (|\psi|^2 - \frac{\mu}{g})^2 + \sum_{i=1}^{\mathcal{N}_o} V_{\mathcal{P}}(\mathbf{r} - \mathbf{q}_i) |\psi|^2 \right] d\mathbf{r}. \quad (5)$$

We now perform DNSs, in which we vary the initial scaled distance r/ξ between the particles; we then obtain $E_{\text{F}}(r/\xi)$, the energy of the minimum-energy state without the SR repulsion, by using the imaginary-time procedure [17]. In Fig. 1 (b) we plot versus r/ξ the potential $U_{\text{A}} = E_{\text{F}}(r) - E_{\text{F}}(r = \infty)$, which is negative (i.e., attractive), for small r/ξ , and vanishes in the limit $r/\xi \rightarrow \infty$.

We can estimate $U_{\text{A}}(r/\xi)$, for the two-particle case, by using the Thomas-Fermi (TF) approximation [18] as follows. We neglect the kinetic-energy term in Eq. (2) and write

$$|\psi(\mathbf{r})|^2 = (\mu - \mathcal{V}_{\mathcal{P}})\theta(\mu - \mathcal{V}_{\mathcal{P}})/g, \quad (6)$$

with $\mathcal{V}_{\mathcal{P}} = V_{\mathcal{P}}(\mathbf{r} - \mathbf{q}_1) + V_{\mathcal{P}}(\mathbf{r} - \mathbf{q}_2)$ and θ the Heaviside function that ensures $|\psi|^2 > 0$. In this approximation,

$$E_{\text{F}}^{\text{TF}} = \frac{1}{\mathcal{A}} \int_{\mathcal{A}} \left[\mu^2 - (\mu - \mathcal{V}_{\mathcal{P}})^2 \theta(\mu - \mathcal{V}_{\mathcal{P}}) \right] / (2g) d\mathbf{r}; \quad (7)$$

$U_{\text{A}}^{\text{TF}} = E_{\text{F}}^{\text{TF}}(r) - E_{\text{F}}^{\text{TF}}(r = \infty)$, which we plot in the inset of Fig. 1 (b) versus r/ξ . It is in qualitative agreement with U_{A} from our DNS; the quantitative difference arises because the TF approximation neglects the kinetic-energy term in Eq. (2).

We now study two simplified cases: (1) head-on collisions, with impact parameter $b = 0$; (2) and collisions with finite, but small b . The schematic diagram in Fig. 2 (a) outlines our procedure. We use an initial state

with two stationary particles O_1 , at $(\pi/2, \pi)$, and O_2 , at $(3\pi/2, \pi)$. We apply the external forces $F_{\text{ext}} = F_0\hat{\mathbf{x}}$ and $F_{\text{ext}} = -F_0\hat{\mathbf{x}}$, respectively, to accelerate the particles; and then we turn off F_{ext} at $t = t_0$ (red vertical line in Fig. 2 (a)). In Fig. 2 (b) we plot versus ct/ξ the x components of the particle velocities $u_{o,x}(t)$, from our DNS with two heavy particles ($\mathcal{M} = 7.5$ and $r_{\text{SR}} = 1.5\xi$), for three different values of the incident kinetic energy E_o . For $E_o = 1.5 \times 10^{-4}$ (blue curves in Fig. 2 (b)), the behavior of $u_{o,x}(t)$ is similar to that of neutral-particle collisions with SR repulsion (Fig. 1 (a)); the collision is completely inelastic and the particles form a bound pair; and the separation between their centers fluctuates around $r \simeq r_{\text{SR}}$. The time average of the velocities of the particles is zero, after the collision. Figure 2 (b) shows that, for $E_o = 1.8 \times 10^{-4}$ (green curves), the two particles rebound, with small non-zero, mean velocities; at the time of the collision, most of the energy is transferred to the repulsive term because of the change in $E_{\text{F}}(t) - E_{\text{F}}(t_0)$ and E_o (see the Supplemental Material [16]). After the collision, most of the energy is transferred back to the fluid and the particles have a small kinetic energy. For higher values, e.g., $E_o = 5.04 \times 10^{-4}$ (magenta curves), the head-on collision between the heavy particles is nearly elastic; and the particles rebound with velocities that are significant fractions of their values at incidence (see the spatiotemporal evolution in Videos M2, M3 and M4 in the Supplemental Material [16]).

We characterize this inelastic-elastic transition by calculating the coefficient of restitution for head-on collisions:

$$e = \frac{u_{2,\text{F}} - u_{1,\text{F}}}{u_{1,\text{I}} - u_{2,\text{I}}}, \quad (8)$$

where $u_{1,\text{I}}$ and $u_{2,\text{I}}$ are, respectively, the mean velocities of the particles O_1 and O_2 before the collision and $u_{1,\text{F}}$ and $u_{2,\text{F}}$ are the mean velocities of these particles after

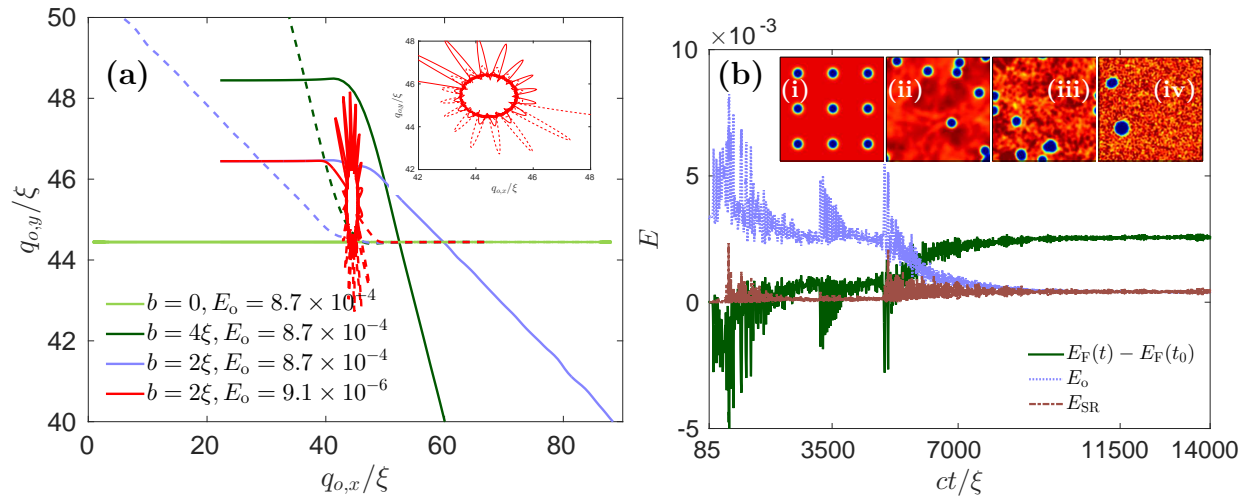


FIG. 3. (Color online) (a) **Collisions at impact parameters $b \geq 0$** : Light green, dark green, and blue curves show the particle trajectories for two heavy particles ($\mathcal{M} = 7.5$) O_1 (solid curves) and O_2 (dashed curves) colliding at $b = 0$, $b = 4\xi$, and $b = 2\xi$, respectively, with incident kinetic energy $E_o \simeq 8.7 \times 10^{-4}$. For $b = 2\xi$ and $E_o = 9.1 \times 10^{-6}$, the colliding particles stick to form a bound pair (red curves); the inset shows an enlarged view of the particle trajectories for the bound-pair, the particle motion is a quasi-periodic function of time. (b) **Aggregation**: Plots of the time evolution of $E_F(t) - E_F(t_0)$, E_o , and E_{SR} for nine heavy particles ($\mathcal{M} = 7.5$) initially placed on a lattice; these are set into motion by the application of constant-in-time forces, random in magnitude and direction, for a short duration $t \leq t_0 \sim 85$. The insets (i)-(iv) illustrate multi-particle collisional dynamics, at the representative times $t_{(i)} = 0 < t_{(ii)} < t_{(iii)} < t_{(iv)}$ by pseudocolor plots of the density field $\rho(\mathbf{r})$; the particles appear as blue disks in which $\rho = 0$.

the collision. For the collisions described above, we find: (1) $e \simeq 0$ for $E_o = 1.5 \times 10^{-4}$; (2) $e \simeq 0.24$ for $E_o = 1.8 \times 10^{-4}$; and (3) $e \simeq 0.68$ for $E_o = 5.0 \times 10^{-4}$. In Fig. 2 (c) we plot e versus E_o from the two-particle, head-on collisions. At low values of E_o , the particle collision is inelastic with $e = 0$; and, as we increase E_o , e becomes finite at a critical value $E_o \simeq 1.6 \times 10^{-4}$, and then there is a steep increase followed by a slow, asymptotic growth towards a value close to 1. We observe a similar inelastic-elastic transition, when instead of E_o , we vary r_{SR}/ξ ; here we consider neutral particles ($\mathcal{M} = 1$) to illustrate that the sticking transition does not necessarily require heavy particles. The plot of e versus r_{SR}/ξ in the inset of Fig. 2 (c), shows that, at low values of r_{SR}/ξ , the particle collision is inelastic with $e = 0$; and, as we increase r_{SR}/ξ , e becomes finite at a critical value $r_{SR}/\xi \simeq 6.46$, and finally attains a value close to 1.

Given the resolution of our study, our data are consistent with a *continuous sticking transition* at which e goes to zero continuously as a power β of the control parameter (either E_o or r_{SR}/ξ). We now give a mean-field calculation of this power-law exponent β . The symmetry of these head-on collisions allows us to write $u_I \simeq -u_{1,I} \simeq u_{2,I}$ and $u_F \simeq u_{1,F} \simeq -u_{2,F}$. The energy balance between the states, before and after the collision, is $E_{\text{rad}}(u_I) + m_o u_F^2 = m_o u_I^2$, where E_{rad} is the energy radiated into sound waves. Therefore,

$$e(u_I) = \sqrt{1 - E_{\text{rad}}(u_I)/m_o u_I^2}, \quad (9)$$

which yields the critical velocity u_I^c at which $e(u_I^c)$ first becomes nonzero. In a simple, mean-field approximation, the Taylor expansion of $E_{\text{rad}}(u_I)$, around $u_I = u_I^c$, yields the mean-field (MF) exponent $\beta^{\text{MF}} = 1/2$. Our DNSs yield values of β that are comparable to, but different from, $\beta^{\text{MF}} = 1/2$. The calculation of β for this sticking transition, beyond our mean-field theory, and its universality, if any, is a challenging problem.

In Fig. 3 (a) we show the trajectories of two heavy particles ($\mathcal{M} = 7.5$ and $r_{SR} = 1.5\xi$) that collide with each other, with an impact parameter $b > 0$. If the incident kinetic energy of the particles is sufficiently high, e.g., $E_o \simeq 8.7 \times 10^{-4}$, they do not stick; the particles get deflected from their incident trajectory at an angle Θ , which depends on b (see Fig. 3 (a) for $b = 2\xi$ and $b = 4\xi$). However, for $b = 2\xi$ with $E_o \simeq 9.0 \times 10^{-6}$, the incident kinetic energy is small enough to allow the formation of a bound pair (red curves in Fig. 3 (a)); the inset shows an enlarged version of the particle trajectories, after the collision, with red solid (dashed) curves for particle O_1 (O_2). The *sun-flower-petal* pattern of these trajectories indicates that, after transients have decayed, the damped, oscillatory motion of the particles in the bound-pair is akin to that of a dimer, with vibrational and rotational degrees of freedom. The power-spectra of the time series $q_{i,j}(t)$, for particle $i \in \{1, 2\}$ and coordinate $j \in \{x, y\}$, show three prominent frequencies, $\omega_a = 0.0185c/\xi$, $\omega_b = 0.0148c/\xi$, and $\omega_c = 0.0222c/\xi$, with $2\omega_a = \omega_b + \omega_c$, i.e., the oscillatory motion is quasiperiodic (data not shown).

If we start with more than two particles, then a suc-

cession of inelastic collisions can lead to the formation of multi-particle aggregates. We illustrate this in Fig. 3(b) for an assembly of 9 particles ($\mathcal{M} = 7.5$ and $r_{\text{SR}} = 1.5 \xi$); to initialize the system, we place the particles on a lattice (inset (i)) and set them into motion by applying constant-in-time forces, with random magnitudes and directions, for a given duration, such that the collisions occur only after the forces are switched off at $t = t_0$. In Fig. 3(b) we plot $E_{\text{F}}(t) - E_{\text{F}}(t_0)$, E_0 , and E_{SR} versus ct/ξ ; large spikes in these plots occur at collisions; subsequent rearrangements into clusters give rise to strong fluctuations in E_{SR} ; as the clusters settle into their optimal configurations, the fluctuations in E_{SR} decrease until they saturate towards the end of our DNS. The pseudocolor plots of $\rho(\mathbf{r})$ in the insets (ii)-(iv) of Fig. 3(b) show the aggregation of particles and the formation of a 7-particle cluster and a dimer (see the spatiotemporal evolution in Video M5 in the Supplemental Material [16]); a much longer DNS should lead to a 9-particle cluster here.

In conclusion, our minimal model of active and interacting particles in the Gross-Pitaevskii superfluid yields qualitatively new results, like the sticking transition and rich aggregation dynamics of particle assemblies. Our qualitative results should hold even in superfluids like Helium, in BECs [19], and in three dimensions. Particles in superfluids have been considered by using Biot-Savart methods [13, 20–22], a two-fluid model [23]; the GPE has been studied with a single spherical particle [11], however, these studies have not considered the collisions and aggregation we elucidate. Impurities in BECs [24] have been described in terms of generalized Bose-Hubbard Models [7], but these works do not study the problems we consider. We hope our work will lead to experimental studies of particle collisions and aggregation in superfluids and BECs.

We thank the Council of Scientific and Industrial Research (India), University Grants Commission (India), Department of Science and Technology (India) and the Indo-French Centre for Applied Mathematics for financial support, and Supercomputing Education and Research Centre, IISc, India for computational resources. V.S. acknowledges support from Centre Franco-Indien pour la Promotion de la Recherche Avancée (CEFIPRA) Project No. 4904. VS and RP thank ENS, Paris for hospitality and MB thanks IISc, Bangalore for hospitality.

* research.vishwanath@gmail.com

† brachet@physique.ens.fr

‡ rahul@physics.iisc.ernet.in;

also at Jawaharlal Nehru Centre For Advanced Scientific Research, Jakkur, Bangalore, India.

- [1] R. J. Donnelly, *Quantized vortices in helium II*, Vol. 2 (Cambridge University Press, 1991).
 [2] G. P. Bewley, D. P. Lathrop, and K. R. Sreenivasan,

Nature **441**, 588 (2006).

- [3] G. P. Bewley, M. S. Paoletti, K. R. Sreenivasan, and D. P. Lathrop, Proc. Natl. Acad. Sci. USA **105**, 13707 (2008).
 [4] G. P. Bewley, K. R. Sreenivasan, and D. P. Lathrop, Exp. Fluids. **44**, 887 (2008).
 [5] D. E. Zmeev, F. Pakpour, P. M. Walmsley, A. I. Golov, W. Guo, D. N. McKinsey, G. G. Ihas, P. V. E. McClintock, S. N. Fisher, and W. F. Vinen, Phys. Rev. Lett. **110**, 175303 (2013).
 [6] M. La Mantia and L. Skrbek, Phys. Rev. B **90**, 014519 (2014).
 [7] N. Spethmann, F. Kindermann, S. John, C. Weber, D. Meschede, and A. Widera, Phys. Rev. Lett. **109**, 235301 (2012).
 [8] T. Frisch, Y. Pomeau, and S. Rica, Phys. Rev. Lett. **69**, 1644 (1992).
 [9] C. Nore, C. Huepe, and M. E. Brachet, Phys. Rev. Lett. **84**, 2191 (2000).
 [10] T. Winiecki, B. Jackson, J. F. McCann, and C. S. Adams, J. Phys. B: At. Mol. and Opt. Phys. **33**, 4069 (2000).
 [11] T. Winiecki and C. S. Adams, Europhys. Lett. **52**, 257 (2000).
 [12] G. E. Astrakharchik and L. P. Pitaevskii, Phys. Rev. A **70**, 013608 (2004).
 [13] E. Varga, C. F. Barenghi, Y. A. Sergeev, and L. Skrbek, J. Low Temp. Phys. , 1 (2015).
 [14] G. D. and S. A. Orszag, *Numerical Analysis of Spectral Methods* (SIAM, Philadelphia, 1977).
 [15] V. Shukla, M. Brachet, and R. Pandit, New J. Phys. **15**, 113025 (2013).
 [16] See Supplemental Material at for the videos and additional figures.
 [17] We prepare such a state by specifying the locations of the particle q_i in Eq. (2), with t replaced by $-it$, and integrate it to obtain the ground state. This procedure yields states whose initial temporal evolution, in the GPE, produces minimal sound emission [25, 26].
 [18] C. J. Pethick and H. Smith, *Bose-Einstein condensation in dilute gases* (Cambridge university press, 2001).
 [19] N. G. Berloff, M. Brachet, and N. P. Proukakis, Proc. Natl. Acad. Sci. USA **111**, 4675 (2014).
 [20] D. Kivotides, C. F. Barenghi, and Y. A. Sergeev, Phys. Rev. B **77**, 014527 (2008).
 [21] D. Kivotides, Y. A. Sergeev, and C. F. Barenghi, Phys. Fluids **20**, 055105 (2008), <http://dx.doi.org/10.1063/1.2919805>.
 [22] Y. Minoda, M. Tsubota, Y. A. Sergeev, C. F. Barenghi, and W. F. Vinen, Phys. Rev. B **87**, 174508 (2013).
 [23] D. R. Poole, C. F. Barenghi, Y. A. Sergeev, and W. F. Vinen, Phys. Rev. B **71**, 064514 (2005).
 [24] A. Klein, M. Bruderer, S. R. Clark, and D. Jaksch, New J. Phys. **9**, 411 (2007).
 [25] V. Shukla, M. Brachet, and R. Pandit, (2014), <http://arxiv.org/abs/1412.0706>.
 [26] C. Nore, M. Abid, and M. E. Brachet, Phys. Fluids **9**, 2644 (1997).
 [27] G. Krstulovic and M. Brachet, Phys. Rev. E **83**, 066311 (2011).
 [28] <http://www.fft.w.org>.

SUPPLEMENTAL MATERIAL

CONSERVED QUANTITIES

We treat the superfluid and particles together as a single system, in which we use the Gross-Pitaevskii equation (GPE) to obtain the spatiotemporal evolution of the condensate wave function $\psi(\mathbf{r}, t)$:

$$i\hbar \frac{\partial \psi}{\partial t} = -\frac{\hbar^2}{2m} \nabla^2 \psi - \mu \psi + g|\psi|^2 \psi + \sum_{i=1}^{\mathcal{N}_o} V_{\mathcal{P}}(\mathbf{r} - \mathbf{q}_i) \psi; \quad (1)$$

here g is the effective interaction strength, m the mass of the bosons, μ the chemical potential, $V_{\mathcal{P}}$ the potential that we use to represent the particles, and \mathcal{N}_o the total number of particles with mass m_o . The equation of motion for the particle i is

$$m_o \ddot{\mathbf{q}}_i = \mathbf{f}_{o,i} + \mathbf{f}_{SR,i} + \mathbf{F}_{\text{ext},i}, \quad (2)$$

where

$$\mathbf{f}_{o,i} = \int_{\mathcal{A}} |\psi|^2 \nabla V_{\mathcal{P}} d\mathbf{r}; \quad (3)$$

$\mathbf{f}_{SR,i}$ arises from the short-range (SR) repulsive potential, $\mathbf{F}_{\text{ext},i}$ is the external force acting on the i th particle, \mathbf{q}_i the particle position vector (the overhead dot represents differentiation with respect to time) and \mathcal{A} is the simulation domain.

In the absence of any external applied force, the total energy E of this system is conserved. We write the total energy of the system as

$$E = E_{\text{F}} + E_o + E_{\text{SR}}; \quad (4)$$

here E_{F} is the energy contained in the superfluid field, E_o the total kinetic energy of the particles, and E_{SR} the energy from the SR repulsion between the particles; these energies are defined, respectively, as follows:

$$E_{\text{F}} = \frac{1}{\mathcal{A}} \int_{\mathcal{A}} \left[\frac{\hbar^2}{2m} |\nabla \psi|^2 + \frac{1}{2} g \left(|\psi|^2 - \frac{\mu}{g} \right)^2 \right] d^2x; \quad (5a)$$

$$+ \sum_{i=1}^{\mathcal{N}_o} V_{\mathcal{P}}(\mathbf{r} - \mathbf{q}_i) |\psi|^2 \Big] d^2x; \quad (5b)$$

$$E_o = \frac{1}{\mathcal{A}} \sum_{i=1}^{\mathcal{N}_o} \frac{1}{2} m_o \dot{\mathbf{q}}_i^2; \quad (5c)$$

$$E_{\text{SR}} = \frac{1}{\mathcal{A}} \sum_{i,j,i \neq j}^{\mathcal{N}_o, \mathcal{N}_o} \frac{\Delta_E r_{\text{SR}}^{12}}{|q_i - q_j|^{12}}; \quad (5d)$$

here \mathcal{N}_o is the number of particles and \mathcal{A} the area of our two-dimensional, computational domain.

The dynamical evolution of the GPE coupled with the equation of motion for the particles Eq. (2)-(3) conserves

the total momentum

$$\begin{aligned} \mathbf{P}(t) &= \mathbf{P}(t=0) + \mathbf{F}_{\text{ext}} t \\ &= \int_{\mathcal{A}} \frac{i\hbar}{2} (\psi^* \nabla \psi - \psi \nabla \psi^*) d^2x + \sum_{i=1}^{\mathcal{N}_o} m_o \dot{\mathbf{q}}_i \\ &+ \mathbf{F}_{\text{ext}} t; \end{aligned} \quad (6)$$

and the total number N of bosons, constituting the superfluid,

$$N = \int_{\mathcal{A}} |\psi|^2 d^2x. \quad (7)$$

PSEUDOSPECTRAL METHOD AND TIME-STEPPING

We use a Fourier pseudospectral method to solve the GPE numerically. Thus the fields in spectral space are obtained through a discrete Fourier transform with a finite number of modes. We introduce the Galerkin projector \mathcal{P}_G

$$\mathcal{P}_G[\hat{\psi}(k)] = \theta(k_{\text{max}} - k) \hat{\psi}(k), \quad (8)$$

where $\hat{\psi}$ is the spatial Fourier transform of ψ , k_{max} is a suitably chosen ultra-violet cut-off, and $\theta(\cdot)$ the Heaviside function. To ensure global momentum conservation we use the 2/3-dealiasing rule, with $k_{\text{max}} = 2/3 \times N_c/2$, where N_c is the number of collocation points [27]. This conservation of momentum is essential for the study of the collision between particles. Thus, the Galerkin-truncated GPE (henceforth TGPE) is

$$\begin{aligned} i\hbar \frac{\partial \psi(\mathbf{r}, t)}{\partial t} &= \mathcal{P}_G \left[\left(-\frac{\hbar^2}{2m} \nabla^2 + g \mathcal{P}_G[|\psi|^2] \right. \right. \\ &\left. \left. - \mu + \sum_{i=1}^{\mathcal{N}_o} V_{\mathcal{P}}(\mathbf{r} - \mathbf{q}_i) \right) \psi(\mathbf{r}, t) \right]. \end{aligned} \quad (9)$$

In our Galerkin-truncation scheme, we can write Eq. (3) as

$$\begin{aligned} \mathbf{f}_{o,i} &= - \int_{\mathcal{A}} \left[\psi^* \mathcal{P}_G[V_{\mathcal{P}}(\mathbf{r} - \mathbf{q}_i) \nabla \psi] \right. \\ &\left. + \psi \mathcal{P}_G[V_{\mathcal{P}}(\mathbf{r} - \mathbf{q}_i) \nabla \psi^*] \right] d^2x. \end{aligned} \quad (10)$$

To perform a direct numerical simulation (DNS) of the TGP Eq. (9), together with Eq. (2) that is coupled with it, we have developed a parallel, MPI code in which we discretize $\psi(\mathbf{r}, t)$ on a square, periodic simulation domain of side $L = 2\pi$ with $N_c^2 = 128^2$ collocation points. We evaluate the linear terms in Eq. (9) in Fourier space and the nonlinear term in physical space; we use the FFTW library [28] for the Fourier-transform operations, and a fourth-order, Runge-Kutta scheme, with time step Δt , to evolve equations Eqs. (2) and (9) in time.

For an assembly of 9 particles (for a full discussion see the Main text), the energy and momentum are conserved upto 2×10^{-5} and 2×10^{-7} percent, respectively; our DNS uses 5×10^6 steps with $\Delta t = 2 \times 10^{-4}$, and $N_c = 128$.

SUPPLEMENTAL FIGURES

Figure 4: Superfluid-mediated attractive potential

Figure 5: Head-on collisions

VIDEOS

Video M1(<https://youtu.be/F3mq-raIdTM>) This video illustrates the collisional dynamics of two neutral particles ($\mathcal{M} = 1$) in the presence of a short-range, repulsive interaction ($r_{\text{SR}} = 1.5\xi$), when they are released from rest. The dynamics of the particles is illustrated by the spatiotemporal evolution of the field $\rho(\mathbf{r})$, shown via sequence of pseudocolor plots, separated by $t = 2.83$ (we use 10 frames per second).

Video M2(<https://youtu.be/2xIUckXILN0>) This video illustrates the collisional dynamics of two heavy particles ($\mathcal{M} = 7.5$) for the incident kinetic energy $E_o = 1.5 \times 10^{-4}$ and $r_{\text{SR}} = 1.5\xi$. The dynamics of the

particles is illustrated by the spatiotemporal evolution of the field $\rho(\mathbf{r})$, shown via sequence of pseudocolor plots, separated by $t = 2.83$ (we use 10 frames per second).

Video M3(https://youtu.be/X5356R4_XwM) This video illustrates the collisional dynamics of two heavy particles ($\mathcal{M} = 7.5$) for the incident kinetic energy $E_o = 1.8 \times 10^{-4}$ and $r_{\text{SR}} = 1.5\xi$. The dynamics of the particles is illustrated by the spatiotemporal evolution of the field $\rho(\mathbf{r})$, shown via sequence of pseudocolor plots, separated by $t = 2.83$ (we use 10 frames per second).

Video M4(<https://youtu.be/fq5HbOPALAs>) This video illustrates the collisional dynamics of two heavy particles ($\mathcal{M} = 7.5$) for the incident kinetic energy $E_o = 5.0 \times 10^{-4}$ and $r_{\text{SR}} = 1.5\xi$. The dynamics of the particles is illustrated by the spatiotemporal evolution of the field $\rho(\mathbf{r})$, shown via sequence of pseudocolor plots, separated by $t = 2.83$ (we use 10 frames per second).

Video M5(https://youtu.be/zqh_3nq-2YY) This video illustrates the collisional dynamics of nine heavy particles ($\mathcal{M} = 7.5$ and $r_{\text{SR}} = 1.5\xi$); initially placed on a lattice and set into motion by the application of constant-in-time forces, random in magnitude and direction, for a short duration $t \simeq 85$. The dynamics of the particles is illustrated by the spatiotemporal evolution of the field $\rho(\mathbf{r})$, shown via sequence of pseudocolor plots, separated by $t = 14.15$ (we use 15 frames per second).

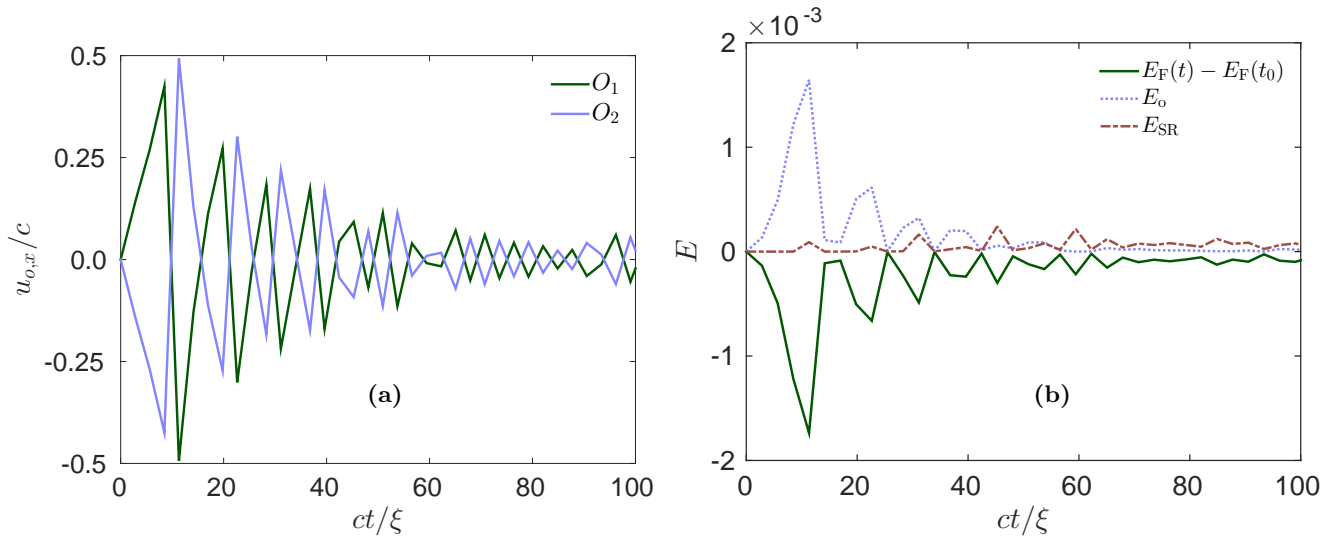


FIG. 4. (Color online) **Superfluid-mediated attractive potential:** (a) Plots of the particle velocity $u_{o,x}$ versus the scaled time ct/ξ ; (b) plots of the time evolution of the energies $E_F(t) - E_F(t_0 = 0)$ (green solid curve), E_o (blue dotted curve), and E_{SR} (magenta dashed curve), following a head-on collision between two neutral particles ($\mathcal{M} = 1$ and $r_{SR} = 1.5\xi$). The particles are released from rest with an initial separation $r_0 = 7\xi$. (For a full discussion see the Main text.)

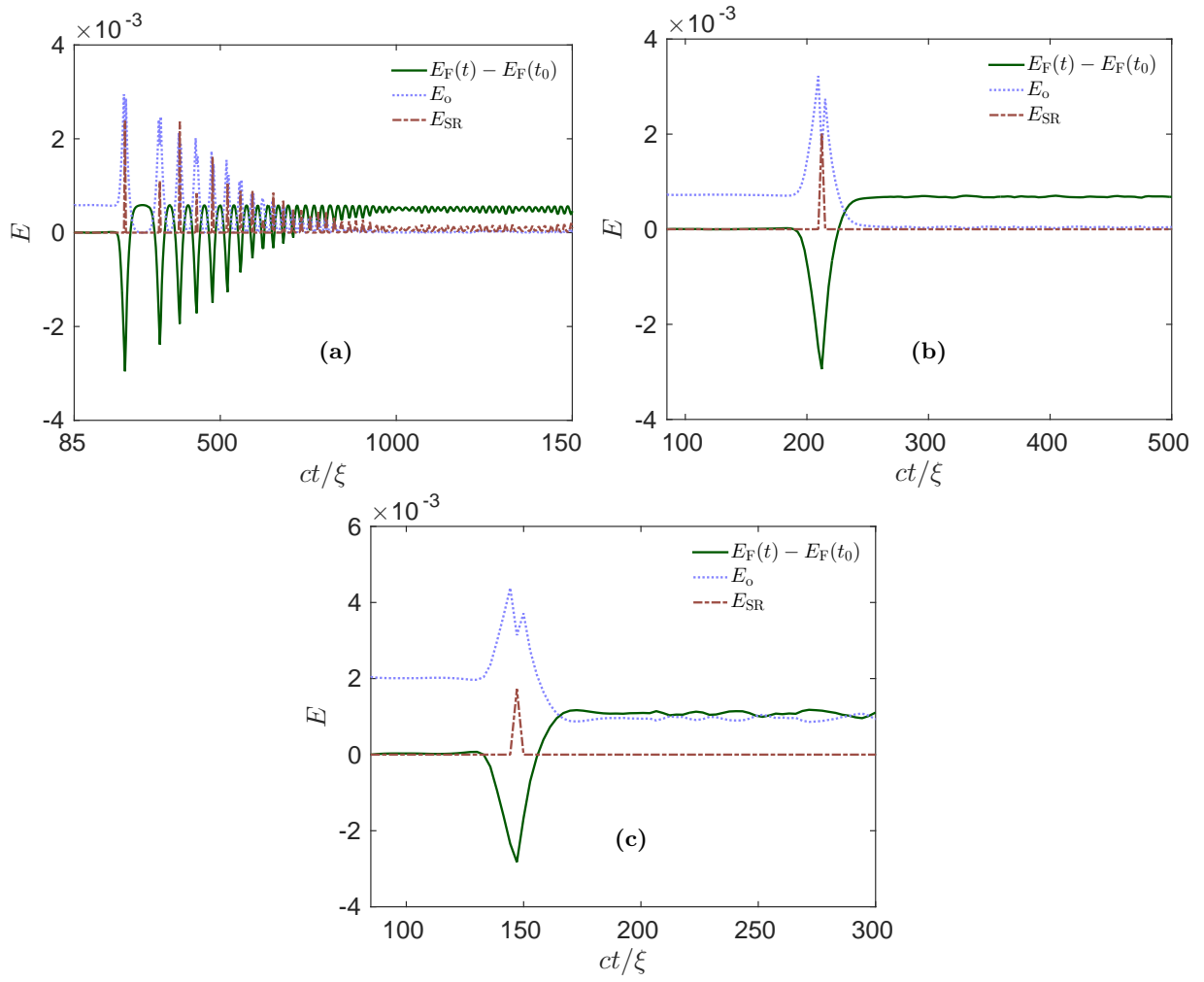


FIG. 5. (Color online) **Head-on collisions:** Plots of the time evolution of the energies $E_F(t) - E_F(t_0 = 85)$ (green solid curve), E_o (blue dotted curve), and E_{SR} (magenta dashed curve) for three different values of the incident kinetic energy (a) $E_o = 1.5 \times 10^{-4}$, (b) $E_o = 1.8 \times 10^{-4}$, and $E_o = 5.0 \times 10^{-4}$, following a head-on collision between two heavy particles ($\mathcal{M} = 7.5$ and $r_{SR} = 1.5\xi$). (For a full discussion see the Main text.)